Control Law Design of the Experimental Aircraft X-31A

H. Beh
G. Hofinger
Deutsche Aerospace AG
Military Aircraft LME212
81663 München
Germany

SUMMARY

This paper presents an overview on the X-31A flight control law design philosophy and the technical realization of the design. After an introduction in the FCS hardware configuration the basic control law structure and the method used for feedback gain calculation are presented. Several elements as the feedforward path, gravity effect compensation, inertial & gyroscopic coupling compensation and the pilot command system are discussed in more detail. Simplified block diagrams of the basic flight control mode in the longitudinal and lateral/directional axis follow. Finally the implementation of the thrust vectoring system including engagement and disengagement procedure is shown.

LIST OF SYMBOLS AND ABBREVIATIONS

AoA	Angle of Attack
A/C	Aircraft
CPU	Central Processing Unit
DASA	Deutsche Aerospace (former Messerschmitt-Bölkow-Blohm MBB)
EFM	Enhanced Fighter Maneuverability
FCC	Flight Control Computer
FCL	Flight Control Laws
FCS	Flight Control System
IMU	Inertial Measurement Unit
IO	Input/Output
LVDT	Linear Variable Data Transducer
PST	Poststall
RI	Rockwell International
TV	Thrust Vectoring

Φ	bank angle
Θ	pitch attitude
α	angle of attack
α_c	angle of attak command
β	sideslip
β_c	sideslip command
δ_{SF}	symmetrical trailing edge command
δ_{DF}	differential trailing edge command
δ_C	canard command
δ_R	rudder command
κ	thrust vectoring command yaw axis
σ	thrust vectoring command pitch axis
$\cos\mu\,\cos\gamma$	direction cosine
$\sin\mu\,\cos\gamma$	direction cosine

J	performance index

V	aircraft speed
g	gravity constant
n_y	lateral load factor
n_z	load factor
p	roll rate body axis
q	pitch rate body axis
r	yaw rate body axis
x_p	pilot command roll axis
x_q	pilot command pitch axis
x_r	pilot command yaw axis

Indices

e	experimental axis
k	nodal line axis (flight path axis)
w	wind axis
c	command

Vectors and matrices

$\underline{p}$	pilot command vector
$\underline{u}$	surface command vector
$\underline{u}_c$	steady state actuator command vector
$\underline{x}$	state variable vector
$\underline{y}$	output vector
$\underline{x}^T$	transpose of vector $\underline{x}$
$\underline{x}_k$	vector $\underline{x}$ @ time k

$\underline{A}$	system matrix
$\underline{B}$	input matrix
$\underline{C}$	output matrix
$\underline{K}$	feedback matrix
$\underline{P}$	Riccati gain matrix
$\underline{Q}$	weighting matrix of performance index
$\underline{R}$	weighting matrix of performance index
$\underline{X}^T$	transpose of matrix $\underline{X}$

INTRODUCTION

The X-31A post stall experimental aircraft was developed to demonstrate enhanced fighter manoeuvrability by using thrust vectoring to fly beyond the stall limit. The goal of the EFM program is to demonstrate the tactical advantage of a fighter aircraft being capable to manoeuvre and maintain controlled flight including the poststall regime up to 70 degrees AoA.

Two fighter type X-31A aircraft were built by Rockwell International and Deutsche Aerospace under contract with the

Advanced Research Projects Agency (ARPA) and the German Ministry of Defense (GMoD).

Since the first flights of aircraft #1 on October 11th 1990 and aircraft #2 on January 19th 1991 the two aircraft have accumulated a total of 400 flights (230 on aircraft #1 and 170 on aircraft #2) as of April 1994. The conventional envelope was cleared to 0.9 Mach, 40 kft pressure altitude, 485 kcas and 30 degrees AoA. Symmetrical loads were cleared between 7.2g's and -2.4g's. Shortly after PST flight test was started both aircraft were transferred from the RI flight test facility at Palmdale Cal. to the NASA Dryden Flight Research Facilities (DFRF) at Edwards Airforce Base to continue the PST envelope expansion flight test (January 1992). Since then more than 200 PST flights have been accomplished and the PST envelope is now cleared up to 70 degrees AoA, between 10 kft and 30 kft pressure altitude, a maximum of 4g's during PST entry and a maximum of 225 kcas entry speed. An extensive tactical flight test to demonstrate the EFM capability of the X-31A aircraft is now the main activity at NASA Dryden. This flight test includes close in combat vs. modern fighter aircraft.

X-31A FLIGHT CONTROL SYSTEM

The X-31A aircraft is a longitudinal unstable (time to double amplitude as low as 200 msec) delta wing A/C with canard configuration. The primary aerodynamic control surfaces are symmetrical trailing edge flaps and canard for the longitudinal axis and differential trailing edge flap and rudder for the lateral/directional axes. In addition a thrust vectoring system is added to the engine exhaust nozzle utilizing three paddles. Each paddle covers an angular section of 120 degrees around the exaust nozzle and can be deflected up to 35 degrees into the plume, leading to a thrust deflection in the pitch and yaw axis of more then 10 degrees. This TV system is used to augment the aerodynamic control power during low speed and PST flight.

The X-31A flight control system is a full authority digital fly by wire system. It consists of three identical FCC's (two CPU's each) supported by a so called tie-breaker FCC. This tie-breaker is like the other FCC's but with just one CPU. It selects the healthy FCC lane in case of a second FCC failure, which gives a quadruplex system reliability. The safety critical flight control components are electrically quadruplex and connected to all four FCC's. These are the pilot inceptors (stick and pedal), the rate gyros, the accelerometers and the actuators of trailing edge flap, canard and rudder. The safety critical actuators (primary control surfaces) are hydraulically duplex. The other components are not considered safety critical, but are necesary to fullfil the EFM requirements and to be able to fly within the PST regime. These are AoA and sideslip sensors located at the noseboom, air data computer, in-
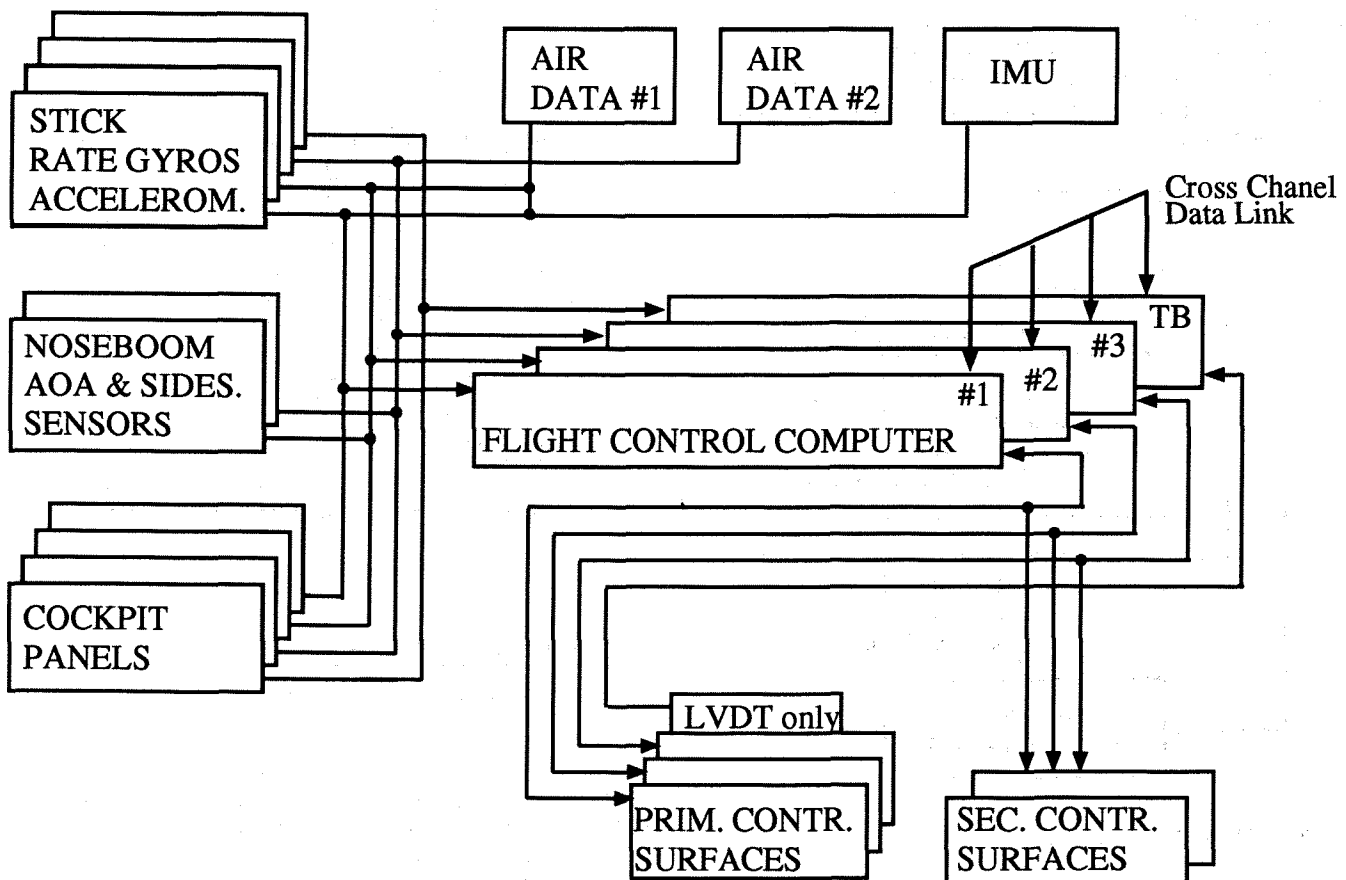

Fig1: X-31A flight control hardware configuration

ertial measurement unit and the actuators of the thrust vectoring paddles, leading edge flap, speedbrake and engine air intake. These components are electrically duplex, except the simplex IMU which has a selftest monitoring feature. The nonsafety critical actuators (secondary control surfaces) are hydraulically simplex. A failure of a nonsafety critical component must be monitored by the redundancy management and reported to the flight control laws. Fig. 1 gives an overview over the flight control system architecture.

In the basic flight control system mode all feedback signals are used to calculate the actuator commands. There are two basic modes, because the TV can be enabled and disabled by the pilot. But PST flight is prevented by the FCL as long as TV is disabled. For takeoff and landing TV is automatically disabled for safety reasons. Depending on the actual sensor failure situation, reversionary modes provide a step by step system degradation, i.e.

- R1 - inertial measurement unit disengage mode

- R2 - flow angle disengage mode

- R3 - fixed gain mode in case of an airdata failure

The most degraded mode, R3, still has save flying home capability. In fig. 2 the step by step degradation is shown; note that the more degraded mode includes the disengagements of the less degraded modes, i.e in R3 mode the IMU and flow angles are also disengaged. The arrows illustrate the possible degradations in case of a hardware failure. The degraded modes are also pilot selectable in a nonfailure situation for flight test purposes.
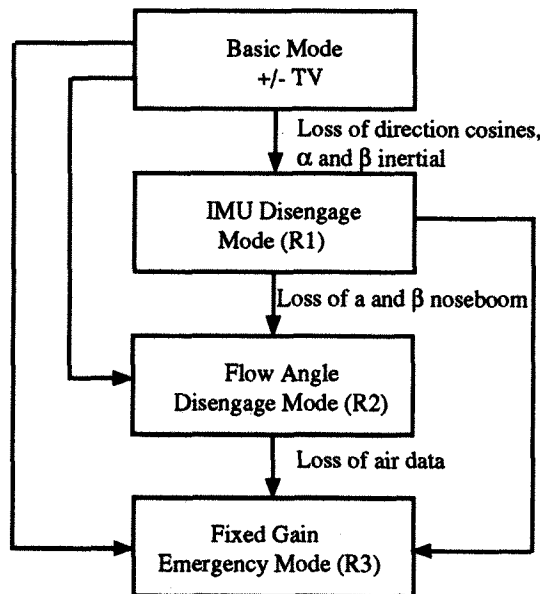

Fig 2: Flight Control System Modes

For safety reasons a spin recovery mode was introduced into the flight control laws. This mode must be selected by the pi-

lot. There are classical direct links from stick and pedal to canard, trailing edge flap, rudder and thrust vectoring, giving the pilot full surface deflection authority. A proportional and integral pitch rate feedback is the only closed stabilization loop in the spin recovery mode.

BASIC STRUCTURE OF THE CONTROL LAWS

The X-31A flight control laws have three main external interfaces i.e.:

the pilot command vector $\underline{P}$ (x_p, x_q, x_r),

the sensed feedback vector $\underline{y}$ (p, q, r, α, β) and

the actuation command vector $\underline{u}$ (δ_{SF}, δ_{DF}, δ_C, δ_R, σ, κ).

Within the PST flight envelope the pilot command vector consists of wind axis roll rate command (x_p), angle of attack command (x_q) and sideslip command (x_r). At high dynamic pressure flight conditions load factor command replaces angle of attack command.
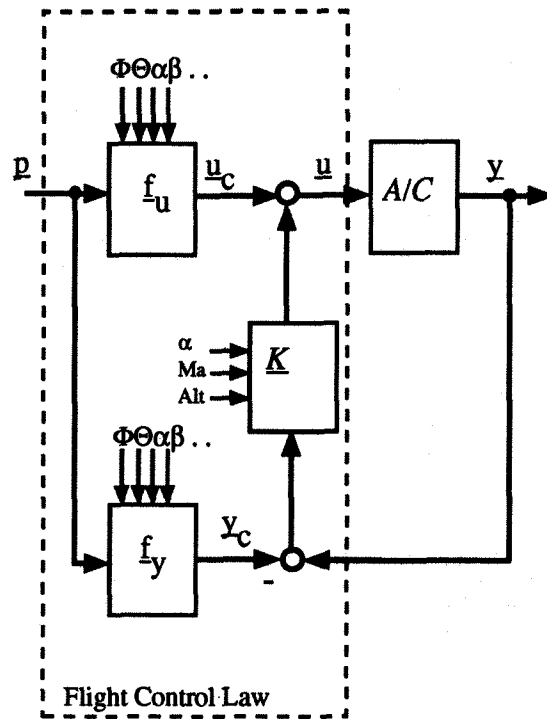

Fig. 3: Basic structure of the X-31A FCL

Fig. 3 shows the X-31A flight control laws in a closed loop together with the aircraft dynamics. There are three subunits within the flight control laws, the linear feeedback unit K and the nonlinear feedforward units f_u and f_y. The feedforward unit f_u calculates the necessary steady state command vector $\underline{u}_c$, i.e. the trimmed surface deflections, for the pilot command vector $\underline{P}$ depending on the actual flight condition and aircraft configuration data (e.g. c.g., weight). In parallel f_y calculates the corresponding steady state command vector $\underline{y}_c$.

543

That means for all feedback signals an associated command signal must be calculated from the pilot input.

The actuator commands are calculated with the following vector equation:

$$\underline{u} = \underline{K} * \left(\underline{y} - \underline{y}_c \right) + \underline{u}_c \quad \text{(Eqn. 1)}$$

Thus the actuator command vector u is the sum of the steady state command vector (trimmed surface deflections) and the feedback difference vector multiplied by the feedback gain matrix.

Determination of the Feedback Gain Matrix K

The feedback gain matrix $\underline{K}$ is determined using the linearised aircraft model split into longitudinal respectively lateral/directional motion. All additional dynamics (e.g actuation and sensor models) are not considered. This leads to fourth order models. Using the z-transform the vector difference equations are
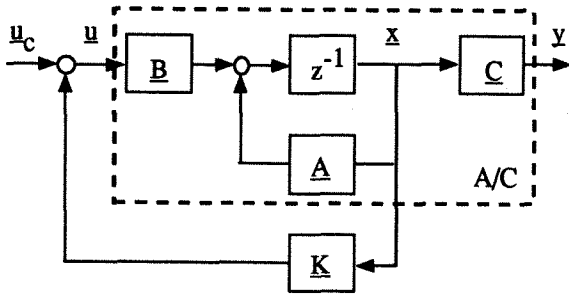
$$\begin{aligned} \underline{x}_{k+1} &= \underline{A}\,\underline{x}_k + \underline{B}\,\underline{u}_k \\ \underline{y}_k &= \underline{C}\,\underline{x}_k \end{aligned} \quad \text{(Eqn. 2)}$$

The feedback matrix is mathematically calculated using the optimal linear digital regulator design. Thereby the main task for the designer is the definition of the weighting matrices $\underline{Q}$ and $\underline{R}$ of the quadratic performance index J (Eqn. 3). The mi-

$$J = \frac{1}{2}\sum_{k=0}^{\infty} \left(\underline{x}_k^T \underline{Q}\,\underline{x}_k + \underline{u}_k^T \underline{R}\,\underline{u}_k \right) \quad \text{(Eqn. 3)}$$

$$\underline{K} = (\underline{B}^T \underline{P}\underline{B} + \underline{R})^{-1}\underline{B}^T \underline{P}\underline{A} \quad \text{(Eqn. 4)}$$

nimization of the performance index for infinite time results in a time constant optimum feedbac: k matrix $\underline{K}$. This matrix is calculated (Eqn. 4) using the system and weighting matrices and the matrix P which is the solution of the "Matrix Riccati Equation" (Eqn. 5). This equation is often referred to as the algebraic Riccati equation.

The stability and handling analysis is carried out with the full high order system. If this check shows unsatisfactory results

the weighting matrices have to be adjusted and the optimization procedure is repeated.

$$\underline{P} = \underline{A}^T \left[\underline{P} - \underline{P}\underline{B}\left(\underline{B}^T \underline{P}\underline{B} + \underline{R} \right)^{-1} \underline{B}^T \underline{P} \right] \underline{A} + \underline{Q}$$

(Eqn. 5)

Calculation of the Feedforward Paths

The feedforward paths are calculated independently from the feedback path using the steady state equations of motion of the aircraft. Steady state is interpreted in this context as the resulting stable flight condition with constant pilot inputs (e.g. steady state wind axis roll). When taking into account all influences in calculating the steady state vectors $\underline{y}_c$ and $\underline{u}_c$, the functions $\underline{f}_y$ and $\underline{f}_u$ describe the inverse steady state model of the aircraft. They include all direct link and all compensation paths (e.g gravity effects, inertial coupling, speedbrake moment compensation ...) and are dependent on configuration and flight condition. Constraints as complexity, model fidelity or computer power do not allow the full implementation of all paths, therefore some of them must be simplified or omitted at all. The steady state feedback difference error is a measurement of this simplification.

Inertial and Gyroscopic Coupling Compensation

The gyroscopic moments are square dependent on the angular rates and therefore not considered in the linearised model. At high angular rates these moments cannot be neglected. Uncompensated these moments would lead to unacceptably large deviations and the aircraft reaction would be lagged by
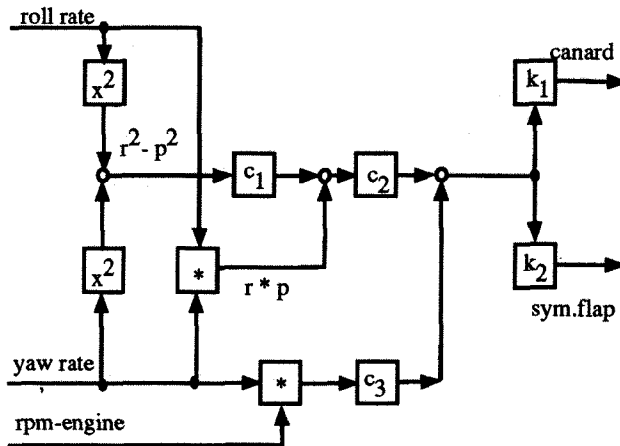

Fig. 4: Inertial & gyroscopic coupling compensation pitch axis.

its dynamic. Introduction of an integral feedback would help, but it introduces overshoots. The better solution is a feedforward compensation acting instantly (just lagged by sensor and actuation dynamics) against the disturbances. The small remaining deviations due to model uncertainties are controlled by the feedback loops. Fig. 4 and fig. 5 show the block diagram of the longitudinal respectively lateral/directional inertial and gyroscopic coupling compensation. The constants c are dependent on the inertias of the aircraft and the engine.

These are used to calculate a normalised compensation moment out of the rates in front of the gains k. These gains are functions of flight conditions. The outputs are the necessary surface deflections to compensate the inertial and gyroscopic moment.
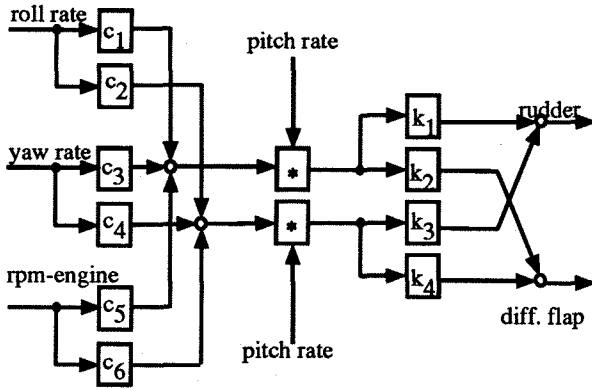

Fig. 5: Inertia & gyroscopic coupling compensation lateral/ directional axis.

Gravity Effect Compensation   The simplest description of the force equation is in the flight path axes system. Here the forces in y- and z-direction (ny and nz) consist just of the centripedal force and the gravity.

$$n_{k_z} = \frac{V_k}{g} q_k + \cos\mu \cos\gamma \qquad \text{(Eqn. 6)}$$

$$n_{k_y} = -\frac{V_k}{g} r_k + \sin\mu \cos\gamma \qquad \text{(Eqn. 7)}$$

They will be used to calculate the flight path rate command signals out of the commanded g's and gravity components.

$$q_{k_c} = \frac{g}{V_k} (n_{k_{z_c}} - \cos\mu \cos\gamma) \qquad \text{(Eqn. 8)}$$

$$r_{k_c} = \frac{g}{V_k} (-n_{k_{y_c}} + \sin\mu \cos\gamma) \qquad \text{(Eqn. 9)}$$

For this the body axes acceleration commands are transformed into flight path axis.

With the dependency of the rates from gravity additional moments due to aerodynamic damping came into the exact equation, the compensation of these moments is neglected.

The time differential of the gravity component leads to angular accelerations. These moments are compensated by a feedforward command.

Additional Control Structure Elements
The simplified model, used for the determination of the feedback matrix, may lead to a high order system with reduced stability and/or degraded handling qualities. With filters in the feedback and feed forward loops this can be improved

again. Failed or missing feedback signals have to be substituted by observers.

If the calculation of the feedforward signals is missing some steady state term (in case of a hardware failure), a steady state error (difference between commanded and sensed signal) will remain. Washout filters in the feedback loop are used to drive this error to zero. Here just the high frequency part of the feedback signal will be used.

Limitations due to loads, control power, sensors and pilot accelerations are kept with scaling and rate limiting of the pilot command loop.

LONGITUDINAL FLIGHT CONTROL LAWS

The pitch stick position is scaled in the flight control laws from -1.0 (max push) to +1.5 (max pull). This position corresponds directly to an AoA or load factor command. At low dynamic pressure flight conditions the FCL is in the AoA comand mode. Here a command of -1.0 corresponds to -10 deg AoA, +1.0 corresponds to +30. deg AoA and +1.5 corresponds to +70. deg AoA. If PST is disabled the AoA command is limited to +30. deg. A force detend in the stick feel system at +1.0 gives the pilot information whether he has pulled into PST or not. At high dynamic pressure -1.0 commands approx. -2.4 g's and +1.0 commands 7.2 g's. Pulling over the detend does not change the maximum command of 7.2 g's (this is the aircraft's load limit). The switch over between these two command systems is at the flight condition where 30 deg AoA results in the maximum load factor of 7.2 g's. This is around 380 psf. Depending on the stick command the associated command is calculated, i.e. in the angle of attack command flight regime the associated load factor command is calculated and vice versa. PST flight is only possible if the aircraft is in the angle of attack command mode.

Fig. 6 presents a simplified block diagram of the longitudinal flight control laws for the AoA command mode. On the left hand side the pilot input (in this case AoA command) and the main feedback sensor signals AoA and pitch rate are shown. The calculated output canard command, symmetric trailing edge flap command and the thrust vectoring command for the pitch axis are on the right hand side. Within the block diagram three areas are surrounded by a dashed line. They reflect the main units as described before.

Direct Link Longitudinal Axis (f_u)
The direct link path in the upper right corner of fig. 6 calculates the steady state canard and trailing edge flap positions out of the commanded angle of attack and the actual flight condition. Derived from trimmed conditions with wings level and max. dry power the according canard and trailing edge flap deflections are stored in a set of two trim-tables. The additional degree of freedom with two control effectors is used to optimize for minimum drag at low angle of attack and lateral stability (aerodynamic stability derivatives are dependant on canard position) at high angle of attack. This set is called the "cruise" trim schedule. But this schedule results in high landing speeds, therefore a second set of trim tables was calculated with the goal of maximum lift at landing angle of attack. This "high lift" schedule is also stored in the flight control

computer. The pilot can switch from one schedule to the other, but the "high lift" trim schedule is restricted for takeoff and landing. For simplification only one set of trim tables is shown in fig. 6.

A lag filter with a time constant corresponding to the angle of attack response of the aircraft is used in front of the trim-tables to compensate the pilot command lead prior to the aircraft response.

The canard and trailing edge deflections to compensate the inertial and gyroscopic moments as defined in fig.4 are added to the output of the trim-tables and this sum forms the steady state trim commands.

The aerodynamic control power is sufficient for trimming, therefore thrust vectoring is not used.

Calculation of pitch rate command (f_v)

The pitch rate command calculation is shown on the left side of fig. 6. First the associated n_z command is derived from the AoA command, using a stored trimmed lift table, dynamic pressure and an estimated aircraft weight. From that the direction cosine of the gravity in the aircraft z-axis is subtracted and multiplication with the gravity constant divided by aircraft speed results in the pitch rate command (Eqn. 8).

Feedback Loops Longitudinal Axis

The feedback loops are shown on the lower right corner of

fig. 6. Inputs are the differences between commanded and actual AoA and pitch rate. These deltas are multiplied by the gains stored in three-dimensional tables as functions of altitude, mach number and AoA and the results are summed up. This sum is a normalised pitching moment the feedback loops ask for. Downstream this pitching moment is distributed with factors to canard, symmetrical flap and pitch axis thrust vectoring command. These factors depend on the flight condition and the actual engine thrust level. They are calculated in the flight control laws using stored tables. There are two different distributions stored in the flight control laws, with and without thrust vectoring. Without thrust vectoring this factor is set to zero and the others are raised accordingly.

It is the designer's choice to select an appropriate distribution of the different pitching moment producers during the optimization of the feedback gains. The $\underline{x}_k$ and $\underline{u}_k$ vector of equation 2 for the longitudinal axis reads:

$$\underline{x}^T = \begin{bmatrix} v_k, \alpha, q, \Theta \end{bmatrix} \quad u = \begin{bmatrix} \delta \end{bmatrix} \qquad \text{(Eqn. 10)}$$

In this equation δ is a linear combination of canard, symmetrical trailing edge deflection and pitch thrust vectoring. For the elements of the performance index weighting matrices only their relative value to each other is important, therefore the control weighting matrix can be set to one. For the state weighting matrix a diagonal matrix was chosen with zeros in the speed and pitch attitude rows. This results in small feed-
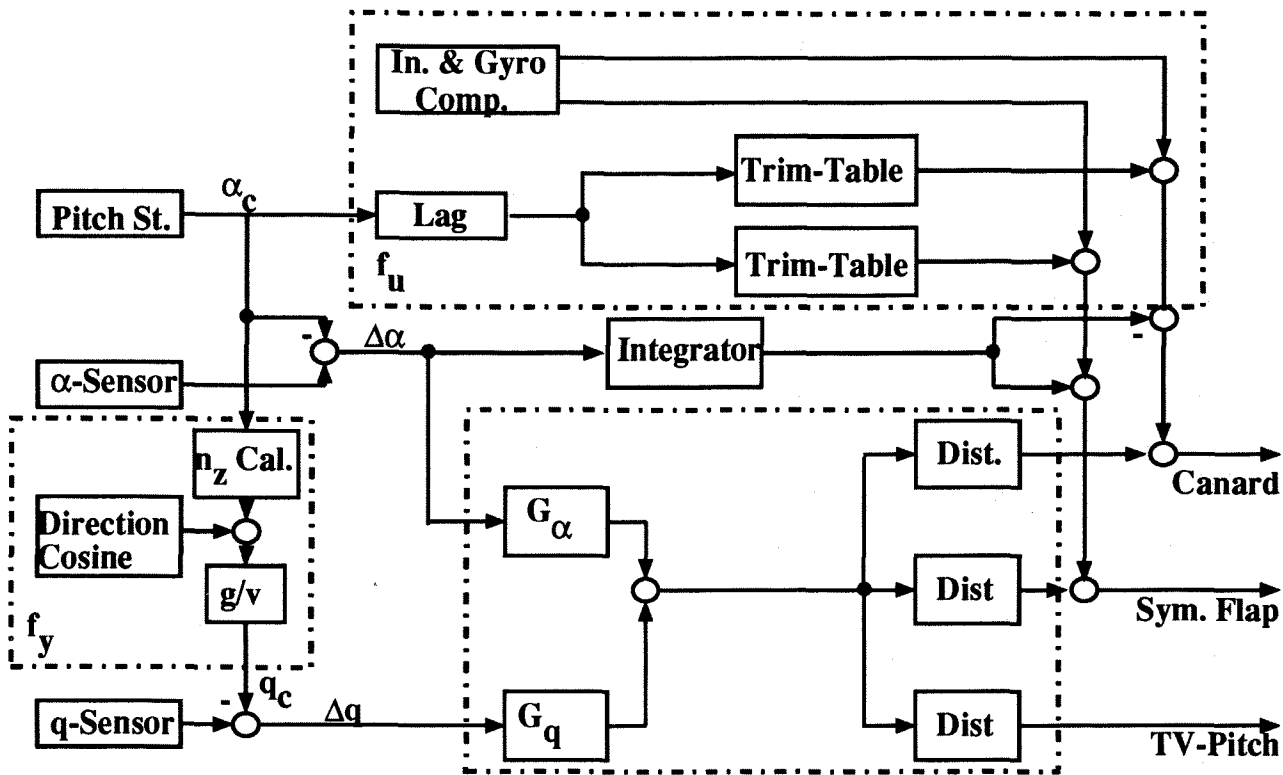

Fig. 6 : Simplified block diagram of the X-31a longitudinal flight control laws. (Basic Mode, α-Command)

back gains for speed and pitch attitude which are neglected because of their small influence on angle of attack motion. The Phugoide cannot be controlled with these feedbacks, but the resulting Phugoide is within the handling quality requirements. The frequency and damping of the angle of attack motion is chosen with the values of q_α and q_q.

$$\underline{Q} = diag\left[0, q_\alpha, q_q, 0\right] \; ; \; \underline{R} = \left[1\right] \quad \text{(Eqn. 11)}$$

In addition an angle of attack resp. load factor error integral is implemented which has not much influence on the angle of attack motion. The Phugoide remains unchanged with angle of attack integral and is more damped with load factor integral.

LATERAL/DIRECTIONAL CONTROL LAWS

Roll stick position is scaled in the flight control laws from -1. (max. left) to +1. (max. right). Depending on the flight condition a maximum wind axis roll command $p_{c\ max.}$ is calculated (up to 240 deg/sec @ low AoA and high dynamic pressure). The maximum roll rate is scaled with flight condition such, that the available control power will be used as much as possible for the steady state roll, with sufficient control power left for stabilization and departure prevention. This maximum command multiplied by the scaled roll stick input gives the wind axis roll rate command p_c.

The rudder pedal command is calculated in a similar way. Here $\beta_{c\ max}$ is calculated as a function of AoA and aircraft speed (up to 12 deg @ low AoA and low speed). This maximum command multiplied by the scaled rudder pedal gives the sideslip command β_c. During rapid rolling the sideslip command is blended to zero, to use the whole control power for rolling (roll priority).

Fig. 7 shows a simplified block diagram of the lateral/directional flight control laws. The large box in the center marked "Gains" represents a matrix multiplication of a combined feedback and feedforward matrix (5 colums, 3 rows) by the input vector (p_c, Δp, Δr, $\Delta \beta$, β_c) resulting in surface commands for rudder, differential trailing edge flap and yaw thrust vectoring.

Direct Link Lateral/Directional Axes (f_u)
In the lateral/directional axis direct links exist from the wind axis roll rate command as well as from the sideslip command to the trailing edge flaps (differential), rudder and thrust vectoring. They are calculated by multiplying the commands with gains. The gains are stored in tables and interpolated depending on flight condition. The direct link commands correspond to the deflections calculated in a steady state flight condition.

The direct link yawing moment is fed to the aerodynamic rudder at angles of attack up to 30°. At post stall conditions the rudder becomes ineffective. Thus direct link is blended to
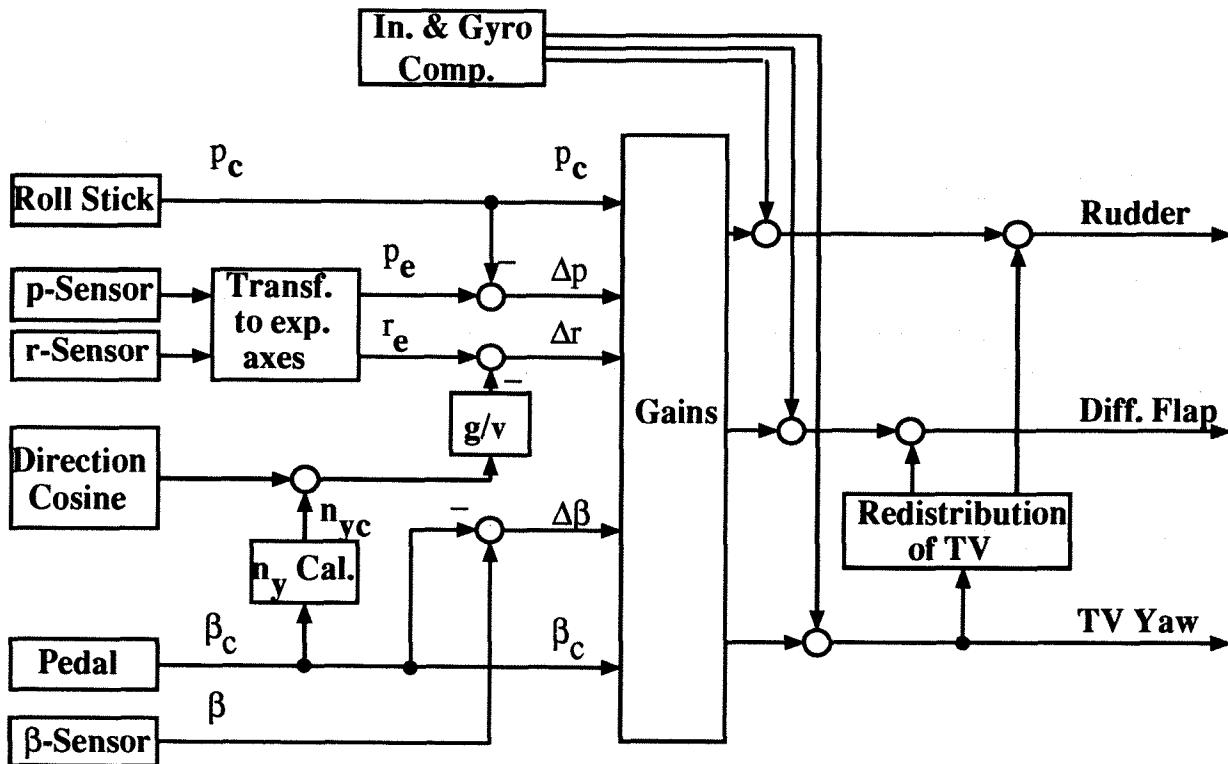

Fig. 7 : Simplified block diagram of the X-31a lateral/directional flight control laws (Basic Mode)

thrust vectoring which takes over the full authority in yaw at 45° AoA.

As with the longitudinal flight control law, the surface deflections to compensate the inertial and gyroscopic moments as defined in fig. 5 are added to the surface commands.

Calculation of yaw rate command (f_{v})

The yaw rate command is not directly a pilot input, thus it has to be calculated in the flight control laws. First the associated n_y command is derived from the sideslip command, using a stored sideforce table, dynamic pressure and an estimated aircraft weight. From that the direction cosine of the gravity in the aircraft y-axis is subtracted and multiplication by the gravity constant divided by aircraft speed results in the wind axis yaw rate command (Eqn. 4).

Feedback Loops Lateral/Directional Axes

Similar to the longitudinal control laws the differences of the commanded and actual sideslip, wind axis roll and yaw rate are multiplied by gains depending on AoA, altitude and mach number. The thrust vectoring gains depend also on estimated thrust. If thrust vectoring is switched off this command is redistributed to rudder and differential flap. Thrust vectoring nearly gives a pure yawing moment, in the stored redistribution tables a combination of rudder and differential flap is precomputed depending on flight condition giving also a pure yaw moment.

The feedback gain matrix is determined by the optimal control theory. The $\underline{x}_k$ and $\underline{u}_k$ vectors of equation 2 for the lateral/directional axes read:

$$\underline{x}^T = \begin{bmatrix} \beta, p_w, r_w, \Phi \end{bmatrix}$$
$$\underline{u}^T = \begin{bmatrix} \delta_{DF}, \delta_R, \delta_{TV} \end{bmatrix}$$

(Eqn. 12)

The weighting matrices are defined as shown below. The Φ-column and -row elements are set to zero and the Φ-feedbacks which have only marginal influence on Dutch Roll and Roll mode are neglected. The diagonal elements of the matrix Q mainly define the eigenvalues of the lateral/directional aircraft motion. The other elements are used to decouple the yawing and rolling motion. The control power is weighted with the diagonal matrix R. A Spiral mode stabilization needs a Φ-feedback or the feedback of an equivalent signal, but the resulting Spiral mode fulfills the handling quality requirements.

$$\underline{Q} = \begin{bmatrix} q_\beta & q_{\beta p} & q_{\beta r} & 0 \\ q_{\beta p} & q_p & q_{p r} & 0 \\ q_{\beta r} & q_{p r} & q_r & 0 \\ 0 & 0 & 0 & 0 \end{bmatrix}$$

$$\underline{R} = \begin{bmatrix} r_{\delta_{DF}} & 0 & 0 \\ 0 & r_{\delta_R} & 0 \\ 0 & 0 & r_{\delta_{TV}} \end{bmatrix}$$

(Eqn. 13)

THRUST VECTORING COMMAND DISTRIBUTION

The longitudinal and lateral/directional flight control systems command effective thrust deflections in pitch and yaw directions. These have to be transformed into the associated vane actuator commands. For this the pitch and yaw commands are transformed into polar coordinates where the maximum effective deflection can easily be limited with engine parameters without changing the direction of the command. Stored thrust vectoring tables depending on desired thrust deflection as well as engine parameters are used to calculate the vane deflections in two steps. First the plume boundary vane position is calculated, then the thrust deflection vane commands are superimposed. At vane deflections larger than 26° geometric clearance is not guaranteed, therefore a software limitation is introduced which allows only one paddle to deflect more than 26°. When thrust vectoring is switched off the two lower vanes (#2 & #3) can be used as airbrakes.
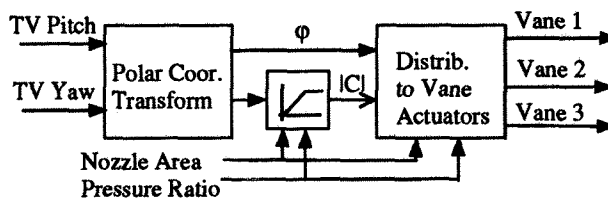

Fig. 8 Thrust vectoring command distribution

ENGAGEMENT/DISENGAGEMENT OF THRUST VECTORING

The thrust vectoring system can be switched on and off by the pilot. In case of a failure thrust vectoring is automatically blended out. This blending is implemented in the flight control software in such a way that the aerodynamic surfaces get additional commands which produce the same overall moment as with thrust vectoring. As long as sufficient aerodynamic control power is available there is no difference in the moments with and without thrust vectoring. With small pilot commands this is valid in the whole conventional flight envelope and for the pitch axis even in the post stall regime. In all these cases the linear handling qualities are nearly unchanged with thrust vectoring in and out. In case of a thrust vector failure in post stall no sufficient yawing moment is available. To keep in this case the sideslip as low as possible, the rudder and the differential flap command is blended out during recovery to low angle of attack. Due to the reduced control power, the roll performance is also reduced with thrust vectoring off.

548

WEIGHT AND THRUST ESTIMATION

For calculation of the load factor command out of the angle of attack command and vice versa as well as for thrust estimation information about the aircraft weight is necessary. For the calculation of the effective thrust deflection information about the aircraft thrust is necessary, because the resulting moment is proportional to the thrust. No sensed signals for weight or thrust are available, therefore these values are estimated with the lift and drag equations which are transformed into body axes. To minimize the dynamic error of these steady state models the following limitations are included:

- lag filters reduce high frequency effects
- the estimations are rate limited
- the estimated values are bounded
- during extreme maneuvres the estimation holds the last value.

The overall accuracy of the estimations depend on the accuracy of the aerodynamic model.

With a new softwareload an engine model was introduced to improve thrust estimation.

POST STALL (PST) MODE

The control law structure does not change with the introduction of the PST-mode. Only the breakpoints in the gain tables and angle of attack dependent scalings are extended to the larger angle of attack range. Flying into the PST is only possible if all of the given prerequisites are fulfilled. If this is the case the pilot can pull to angles of attack larger then 30°. To prevent the pilot from unintentional PST entries a detent is introduced in the stick force spring at 30° angle of attack command. If one or more of the prerequisits are not longer fulfilled, or in case of a failure the angle of attack command is automatically reduced to 30°.

CONCLUDING REMARKS

Flight test confirmed the design approach and the control law structure concept including the thrust vectoring system to be successful. The aircraft dynamics were rated by the pilots close to existing level 1 handling quality requirements throughout the whole conventional envelope. Within the post stall envelope no settled requirements exist, however the pilots rated the handling and performance of the airplane as excellent, impressive and well satisfactory.

During the last two years of flight test no significant control law structure changes were necessary. The only major modification was the introduction of limited integral feedbacks of sideslip and roll rate error. This was necessary due to unpredicted large asymmetries in the lateral/directional axis encountered during flight test at AoA's greater than 40°.

Two updates of the aerodynamic model shortly before first flight and during flight test showed the flexibility of the optimal control approach. This was demonstrated by a redesign of the feedback gains performed in less than one month.

549